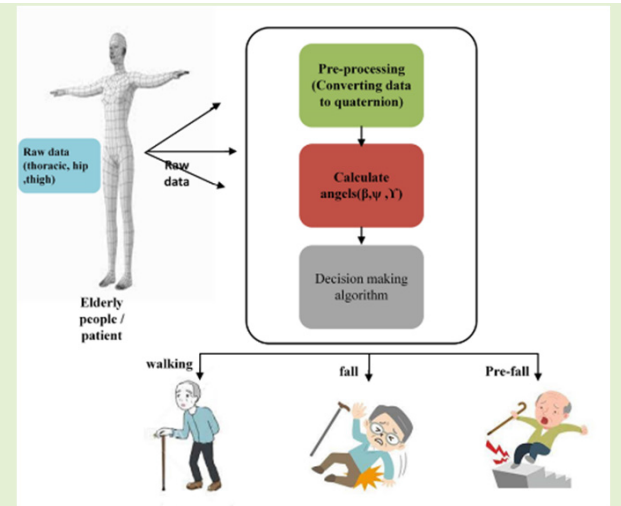


# A Mathematical Model for Fall Detection Prediction in Elderly People

Safa Hussein Mohammed<sup>✉</sup>, Yangyu Fan<sup>✉</sup>, Guoyun Lv<sup>✉</sup>, and Shiya Liu<sup>✉</sup>

**Abstract**—The falling risk of elderly people has become a significant issue. The use of a single sensor to detect the falling was found ineffective. Hence, methods such as video detection and use of more sensors were investigated, and falling prediction based on human body kinematics (HBK) and motion was studied. The model consisted of two algorithms: a prediction algorithm to predict the occurrence of a fall from daily activity living (DAL) and a decision-making algorithm to classify the DAL (fall or no fall). The model was analyzed using three inertial measurement unit (IMU) sensors with three degrees of freedom (DOF) that were assumed to be set on the thoracic, hip, and knee joints. The model used quaternions to represent the orientation of the three joints. To determine the occurrence of a fall, the joint angles for the thoracic, hip, and knee were calculated, and the world frame was used as a reference and a T-pose skeleton for coordinate calculation. The proposed model was evaluated using a ready-made dataset called IMU dataset; which contains real-time human motion obtained from IMU sensors. The evaluation was done using MATLAB simulation. The outcomes of the evaluation show that the proposed model is efficient and promising.

**Index Terms**—Fall detection, human body kinematics (HBK), no-fall, degrees of freedom (DOF), sensor.



## I. INTRODUCTION

FALLS among elderly individuals over the age of 60 are regarded as a significant health issue. The World Health Organization (WHO) reports that between 28% and 35% of individuals aged 65 years and older experience falls each year [1]. Shockingly, falls are the second most common cause of death [2] and in fact, approximately 40% of all injury-related deaths among the elderly are due to falling.

Muscle weakness in elderly people makes them especially susceptible to the lasting effects of falls. Fall risks are elevated

for the elderly because of weakened leg muscles. This makes elderly people, more likely to suffer from long-term injuries like sprains, fractures, and concussions. There is a shortage of nursing care professionals at a time when the number of elderly people with walking dysfunctions is rising [3].

Various approaches to analyzing human motion have been used in the past. In the field of kinesiology, there has not been a kinematics and kinetic examination of the entire body in motion. It is now possible to calculate the joint forces and moments of force for each instantaneous position of full-body motion using high-speed photography, anatomical information, and mechanics. For many years, kinetic evaluations of one or two segments of prosthetic devices have been performed [4], but the entire body has not been subjected to these analyses. In [5], Tasmanian recorded a few movements using electromyography, while in [6], studied the kinematics of a few joints. By measuring the joint moments of force of whole-body activities, movement, on the other hand, may be better understood. The data collected can be used in sports, therapy, and other industries that require body motion analysis. The method can be used to evaluate a person's performance in real-world competitions as well as laboratory-controlled movements [7]. The human motion system is a

Manuscript received 24 July 2023; revised 22 August 2023; accepted 23 August 2023. Date of publication 19 September 2023; date of current version 16 October 2024. This work was supported in part by the Key Program of Research and Development Plan of Shaanxi Province under Grant 2020ZDLGY04-09 and in part by the Department of Science and Technology of Shaanxi Province. The associate editor coordinating the review of this article and approving it for publication was Prof. Rosario Morello. (*Corresponding author: Guoyun Lv*)

Safa Hussein Mohammed, Yangyu Fan, and Guoyun Lv are with the School of Electronic and Information, Northwestern Polytechnical University, Xian, Shaanxi 710072, China (e-mail: safahussein@mail.nwpu.edu.cn; fan\_yangyu@nwpu.edu.cn; lvguoyun102@163.com).

Shiya Liu is with the Content Production Center of Virtual Reality, Beijing 100036, China (e-mail: shiya.liu@cpcvr.org.cn).

Digital Object Identifier 10.1109/JSEN.2023.3309646

complex network, consisting of approximately 204 bones, 78 joints, over 600 muscles, and more than 200 degrees of freedom (DOF), as detailed in [1]. Advanced sensors can precisely quantify the postural metrics of a single limb during movements, as illuminated in [8].

Classifying human motion has also been done using image-processing techniques in recent years. Human posture can be defined in images captured by a wide variety of imaging modalities using learning-based algorithms [9]. These classification algorithms evolved out of earlier methods like machine learning and deep learning. In addition, sensors that can detect human joints have become increasingly popular for understanding human posture. One of the most popular sensors is Microsoft's Kinect [9]. It is not a wearable device, but rather uses infrared light to detect joints and sends that data to a computer via a USB cable, making it ideal for this purpose. Many robotic canes and other walking aids have been proposed as ways to help the elderly and disabled get more exercise.

They describe a new real-time method for tracking daily activities and detecting falls [10]. Movement patterns are classified into two types: complex fall and non-fall. A single triaxial accelerometer attached near the waist collects movement data. In the literature, threshold-based algorithms are frequently described.

Most of them employ multiple features at once, such as accelerating in Cartesian space based on the user's orientation [11]. Note that not all autumnal patterns follow this rule. An alternative method is to set off both the magnitude  $r$  and the orientation [12]. Magnitude  $r$  is superior to independently activating each axis because it takes into account the energy of all possible fall directions. A spherical coordinate component,  $r$ , is the magnitude [10].

In [13], they proposed a system for detecting falls by classifying different activities as fall or non-fall actions and alerting the elderly person's relative or caregiver in the event of an emergency.

In [14], a new and improved method for detecting falls based on depth is mentioned. Their method, which uses a shape-based characterization of falls and a support vector machines (SVMs) classifier, is intended to distinguish falls from other common occurrences. For a more accurate description of a fall's general form, we employ a combination of curvature scale space (CSS) features and fisher vector (FV) encoding. The bag-of-words (BOWs) model is replaced with FV encoding because of its superior performance.

When using simple linear classifiers, the FV representation keeps working effectively and reliably. The correct and effective classification of people's posture is the subject of numerous ongoing and future studies, particularly in the field of health [15].

Various studies on fall detection and its alteration were investigated in the literature [16]. However, there have been few studies on a prediction fall. In this article, we developed a mathematical model that can predict the portability of fall occurrence based on human body kinematics (HBK) as well as using quaternions to present the rotation of three joints (thoracic, hip, and knee). The model can implement both online and offline in real-time.

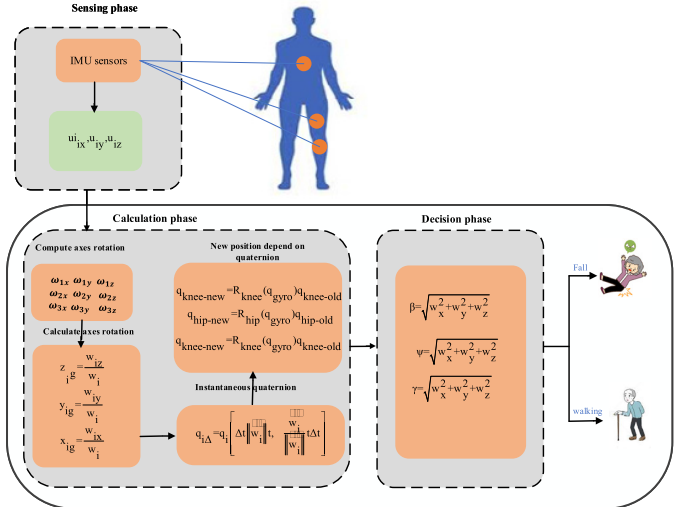


Fig. 1. Block diagram for the proposed mathematical model.

The developed model is divided into two parts: a fall prediction algorithm that predicts the likelihood of the human falling, and a decision-making algorithm that classifies the human or patient as falling or not falling. The prediction algorithm predicts the fall depending on the joint angles of three joints (thoracic, hip, and knee); to calculate the joint angles, there are two methods: the first is to calculate the joint angle with the next joint as a reference, and the second is to calculate all joint angles with one reference. In this developed model, we used the second method, which is to calculate all joint angles with one reference point (the center of the hip) as the reference point.

The range of motion and degree of rotation of a joint is directly related to the mobility of a human being because joints are pivotal components of the skeleton. Because of our one-of-a-kind skeletal architecture, joint movement patterns and rules are limited. Our bodies only have joints that can rotate, not move in other directions (translate). Additionally, there is a cap on the range of motion and the normal rotation angle of each joint [8].

In humans, there are six different types of joints based on their shape: the trochlear joint, the elliptical joint, the saddle joint, the ball-and-socket joint, the pestle-and-mortar joint, and the plane joint [8]. The amount of rotational freedom available in different types of joints varies. Different types are distinguished by the number of DOF the joint has for rotation: uniaxial, biaxial, and multiaxial [8].

The rotation of a joint is defined as the rotation of the distal limb relative to the proximal limb [8]. In this developed model, the joint angles of rotation were calculated using the center hip as a reference.

According to research, the upper trunk is the best feature region for distinguishing falls from other movements by acceleration [17]. In this article, the model developed was based on the upper and lower limbs to assist the elderly falling (see Fig. 1). Three detection places of the thoracic, hip, and knee were investigated (Fig. 2). Quaternions are used to represent the orientation in this model.

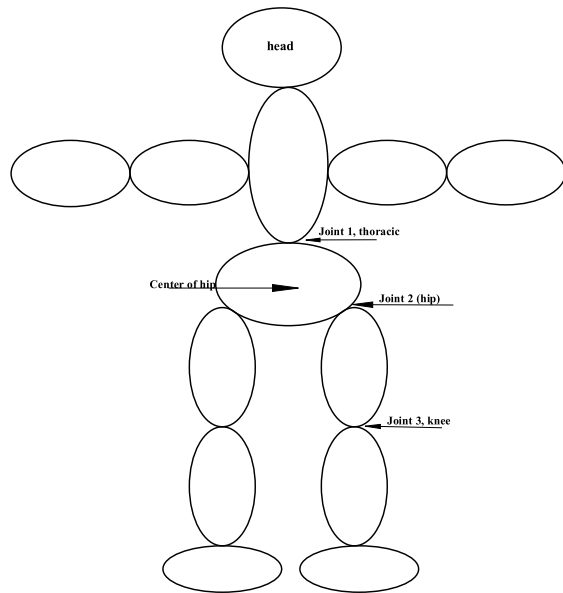


Fig. 2. Show sensors sat on three joints (thoracic, hip, and knee).

The remainder of this article is divided into five sections. The purpose of this study is briefly mentioned in the Section I. Section II presented the mathematical prediction model and hypotheses for the model, the methodology and method strategy, and information about the methods used in this study. Section III presented the model evaluation, as well as the algorithm employed in the developed model; and contains a discussion section as well as the results. Finally, there is a conclusion title in the Section IV that summarizes the study.

## II. MATHEMATICAL PREDICTION MODEL

The hypotheses and methodology strategy and structure used to develop the mathematical prediction model are described in this section.

### A. Quaternion

The angular position of a particular reference frame can be ascertained in relation to another frame of reference using a set of parameters known as a quaternion. This correspondence can be represented in several distinct forms, some of which are easier to comprehend than others, although each has its own set of limitations. Rotation matrices, Euler angles, and quaternions are typical illustrations. The angular attributes of a body can be incessantly estimated through orientation or attitude monitoring systems, which rely on precise measurements [18].

A quaternion is a type of hypercomplex number that exists in four dimensions and is used to elucidate the orientation of space using complex numbers. Unlike Euler angles, the problem of singularities is absent in quaternions; they are capable of describing a full attitude, and their application does not necessitate a considerable number of trigonometric operations. Furthermore, unlike a rotation matrix, the quaternion does not encompass any superfluous variables, resulting in reduced memory requirements and increased computational efficiency. Moreover, quaternions offer some benefits that Euler angles and rotation matrices lack, including easy smoothing and interpolation, and are an

essential element in motion synthesis and reuse. As a result of these advantages, quaternions find extensive application in computer animation, attitude resolution, and control [19]. As a 4-D vector, a quaternion is a four-element complex [8]. From [8], [18], and [19], we can write

$$q = \begin{bmatrix} q_0 \\ q_1 \\ q_2 \\ q_3 \end{bmatrix} \quad (1)$$

where  $q_0 q_1 q_2 q_3$  are real numbers when a quaternion is used to express attitude or rotation, it must be a unit quaternion, that is,  $\|q\| = 1 \cdot q_0$  is the scalar part of the quaternion  $q$  is the vector part of the quaternion.

The rotation is performed through the double quaternion multiplication given by (5)

$$\vec{p} = q \vec{u} q^*. \quad (2)$$

Here,  $q^*$  designates the complex conjugate of the quaternion  $q$ . In line with Euler's rotation theorem, rotational movement can be executed by rotating an angle around a specific rotation axis. Presume the rotation axis to be the unit vector and  $\theta \in R^3$  as the angle of rotation. By leveraging the rotation axis  $\vec{u}$  and  $\theta$  the rotation angle, the body's posture can be established according to the following equation:

$$q = \left( \cos \frac{\theta}{2}, \vec{u} \sin \frac{\theta}{2} \right). \quad (3)$$

The utilization of transformation composition represents one of the pivotal advantages inherent in quaternions. Specifically, transformation composition finds widespread application in the manipulation of the human body due to its capacity to impact child joints and bones. Given these circumstances, employing quaternions to represent the state of a joint offers numerous benefits. This is largely due to the uncomplicated process whereby one can restore the rotation axis and angle from the quaternion. As a professional spelling and grammar corrector and improver, I have made minor edits to ensure grammatical accuracy [18].

### B. Model Structure

The developed model encompasses three primary stages (refer to Figs. 3 and 4): initially, the collection of data and the precreation of parameters to enable the analysis and selection of variables from elderly individuals/patients (sensing stage), followed by a phase of calculation and determining to forecast the probability of a fall incidence, and finally culminating in the decision-making stage.

**1) First Phase:** This phase involves the input data, which was collected from elderly people or patients using the previously mentioned wearable sensors and inertial measurement unit (IMU) sensors located on the human body (see Fig. 1). The sensors measure angles  $\theta$ ,  $\phi$ , and  $\alpha$ ; where  $\theta$  is the rotation angle for the thoracic joint,  $\phi$  is the rotation angle of joint number two (hip), and  $\alpha$  is the rotation angle of joint number three (knee). When  $\theta$  is a 3-D vector for joint one (thoracic)  $\theta = [\theta_x \theta_y \theta_z]$ ; where  $\theta_x$  represent rotational body angular velocity around the  $x$ -axis (roll),  $\theta_y$ ,  $y$ -axis (pitch),

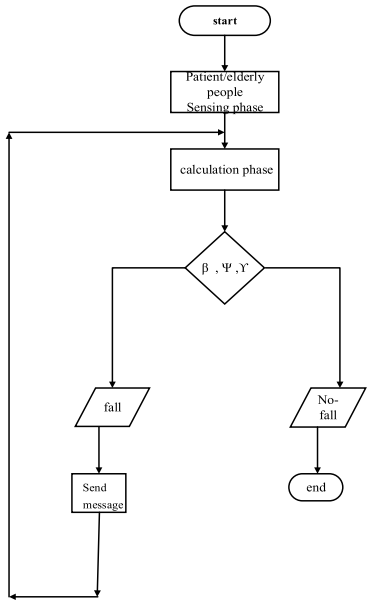


Fig. 3. Mathematical model flowchart.

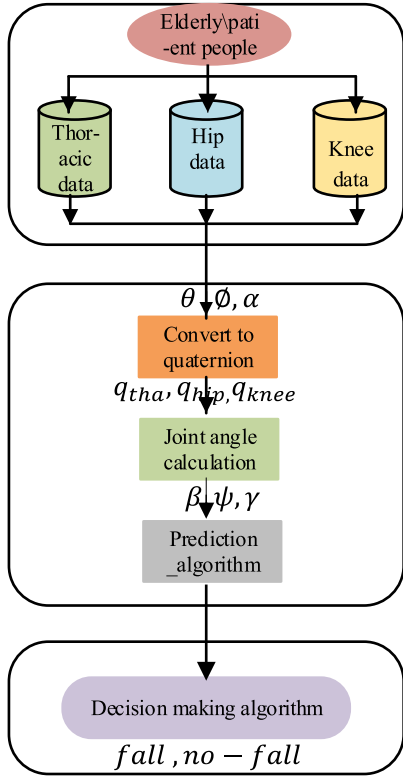


Fig. 4. Data flow for a Mathematical Model.

and  $\theta_z$ ,  $z$ -axis (yaw)),  $\phi$  is a 3-D vector for joint two (hip)  $\phi = [\phi_x \phi_y \phi_z]$  where  $\phi_x$  represent rotational body angular velocity around the  $x$ -axis (roll),  $\phi_y$ ,  $y$ -axis (pitch),  $\phi_z$ ,  $z$ -axis (yaw).  $\alpha$  is a 3-D vector representing the angular velocity for joint three (knee)  $\alpha = [\alpha_x \alpha_y \alpha_z]$ ; where ( $\alpha_x$  represent rotational body angular velocity around the  $x$ -axis (roll),  $\alpha_y$ ,  $y$ -axis (pitch), and  $z$ -axis (yaw)).

We assume the system has an output signal as follows [20]:

$$Y(X) = F(X) + \varepsilon \quad (4)$$

where

- |                                     |  |
|-------------------------------------|--|
| $Y(x)$                              | predicting output;                                 |
| $X$                                 | input data composed $n$ data of three IMU sensors; |
| $\varepsilon \sim N(0, \sigma_0^2)$ | Gaussian observation noise.                        |

To predict the outputs that represent the fall and no-fall from the input data, we do some calculations in the input data. The joint's angles of rotation are calculated for one reference. The reference is the hip center. At each step or movement [fast step (FS) or slow step (SS)], sensors measure the rotation angles  $\theta, \phi$ , and  $\alpha$  which are considered inputs to the second phase of the model. In this model, only the rotational DOF of the joints are considered.

**2) Second Phase:** The human body's coordinate system: The movement of each skeleton relative to its parent skeleton can be explained by utilizing the human body's coordinate system. Since each skeleton can only move relative to its parent skeleton, each one necessitates its individual human body coordinate [8]. In this model, the T posture skeleton was employed for the coordinates. In order to be monitored, each skeleton and joint requires its own distinctive local coordinate system to depict its motion states [21]. The spinal column and pelvis constitute the core of the thoracic bone coordinate system. In an upright position of the upper body, the  $X$ -axis signifies the forward direction, the  $Y$ -axis aligns with the spinal cord up to the cranium's top, and the  $Z$ -axis is positioned on the right-hand side. The center of the hip joint is employed to define the coordinate system for the thigh. The thoracic, hip, and knee joints were utilized for the model (refer to Fig. 2). This article elucidates the local coordinate system of several major bones as an explicit mechanism to describe the body's coordinate system. In particular, the trunk skeleton constitutes the amalgamation of the rib cage skeleton coordinate system and the pelvic skeleton coordinate system. On the other hand, the thoracic bones form an integral component of a broader coordinate system that encompasses both the spinal column and the pelvis. In cases where the head and shoulders maintain a vertical alignment, the body's axes adopt the following configuration: the  $X$ -axis denotes the forward direction, the  $Y$ -axis spans the spinal column until the pinnacle of the cranium, and the  $Z$ -axis is situated at the right-hand side of the body. The central axis of the pelvis lies precisely at its core. In instances involving an individual exhibiting T-standard posture, the orientation of the upper limb coordinate system is identified by the  $X$ -axis pointing in the anterior direction, the  $Z$ -axis indicating the upper limb's right-hand side, and the  $Y$ -axis traversing along the body's vertical axis. Coordinate systems are established at the hip, knee, and ankle using the center of rotation for each limb as its corresponding origin point. The lower limb coordinate system is distinguished by an  $X$ -axis pointing forward while the limb is at rest and a  $Z$ -axis positioned toward the right-hand side [22]. To institute a segment's rotation, one must initiate with the right horizontal axis and subsequently turn counterclockwise around the segment's present location. The segment's angular displacement is indicated by the quadrant in

which it is situated. Upon clockwise rotation of the segment, the sign of the angular acceleration would be reversed [7] (Fig. 5).

**3) T Pose:** There are several methods for defining the initial stance and allotting axes to individual joints. The most straightforward approach involves beginning with a T pose and subsequently attaching axes to each joint in a manner such that the Z-axis points forward. Axes are not required for the endpoints, including the wrists and feet, since the orientation of each joint is determined solely by its parent's rotation matrices (see Fig. 6). In standard posture, the lower limb coordinate system is characterized by a vertical Y-axis running up along the lower limb, an X-axis orienting straight ahead, and a Z-axis indicating toward the right-hand side [22].

According to [23], the rotation matrix between two adjacent body segments was computed as follows:

$${}^{b_I}R_{b_J} = ({}^{\text{ref}}R_I{}^I R_{b_I}) {}^{\text{ref}}R_I{}^J R_{b_J} \quad (5)$$

where  $b_I$  and  $b_J$  are the proximal and distal body segments and the  ${}^{\text{ref}}R_I$  is the quaternion-derived rotation matrix representing the  $I$ -sensor orientation, i.e., the relative rotation between the  $I$  and the world reference system (ref)

$$R = \begin{bmatrix} q_0^2 + q_1^2 - q_2^2 - q_3^2 & 2(q_1q_2 - q_0q_3) & 2(q_1q_3 - q_0q_2) \\ 2(q_1q_2 + q_0q_3) & q_0^2 - q_1^2 + q_2^2 - q_3^2 & 2(q_2q_3 - q_0q_1) \\ 2(q_1q_3 - q_0q_2) & 2(q_2q_3 + q_0q_1) & q_0^2 - q_1^2 - q_2^2 + q_3^2 \end{bmatrix}. \quad (6)$$

The calculations phase of the model begins with converting the data collected from human body measurements using IMU sensors ( $x$ ) into quaternions (27). (Each data point in the input (sensor data) is represented by  $q_i = [q_{i1}^T, q_{i2}^T, q_{i3}^T \dots, q_{in}^T]$  where  $i$  the number of the sensors; in our model, the number of sensors is three; from  $i = 1, 2, 3$ . A quaternion can be used to describe single-limb posture; in our model, we used three quaternions to represent the three joints at the thoracic, hip, and knee. Using (2), (6), (7), and (19), we can write

$$q_{\text{tha}}(t) = \begin{bmatrix} a_0 \\ a_1 \\ a_2 \\ a_3 \end{bmatrix} = (\cos(\theta)t, \vec{a} \sin(\theta)t) \quad (7)$$

$$q_{\text{hip}}(t) = \begin{bmatrix} b_0 \\ b_1 \\ b_2 \\ b_3 \end{bmatrix} = (\cos(\phi)t, \vec{b} \sin(\phi)t) \quad (8)$$

$$q_{\text{knee}}(t) = \begin{bmatrix} c_0 \\ c_1 \\ c_2 \\ c_3 \end{bmatrix} = (\cos(\alpha)t, \vec{c} \sin(\alpha)t) \quad (9)$$

where  $\theta, \phi, \alpha$ , are measured velocity angles in rad/sec in each movement (time) from IMU sensors (gyroscope) from three joints; thoracic joint, hip joint, and knee joint, respectively  $t$  is time.

Calculate the angles  $\psi, \beta$ , and  $\gamma$ (31), which represent the rotation joint angles of the thoracic angle, hip angle, and knee angle. We calculate the angles in each movement ( $t$ ). The

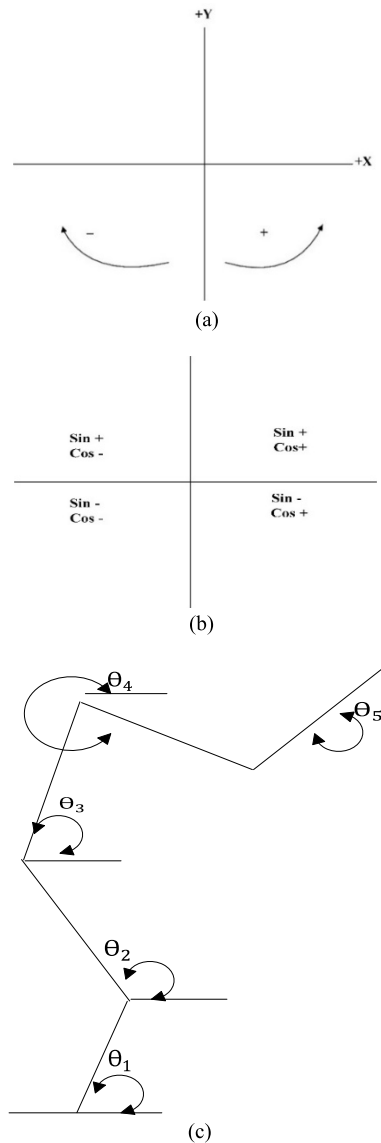


Fig. 5. (a) Absolute motion method and (b) sign of the movement segment in human [7] motion [18].

model has ability to predict the situation of human falls and non-falls.

The individual's condition is determined based on the joint angle of rotation values for the three joints, as indicated in Table I. The range of motion for the knee joint is demonstrated for various activities of daily living (ADL) in the measurement.

**To calculate the joint angle of rotation for the three joints following steps are implemented: from (1) and (3).**

- 1) The IMU reading the data (velocity in rad/sec)  $[u_{ix}, u_{iy}, u_{iz}]$ ;  $i = 1, 2, 3$ .
- 2) Then, we compute the axes of rotation  $(x_{ig}, y_{ig}, z_{ig})$

$$x_{ig} = \frac{w_{ix}}{w_i}, \quad y_{ig} = \frac{w_{iy}}{w_i}, \quad z_{ig} = \frac{w_{iz}}{w_i}. \quad (10)$$

- 3) Start from the initial quaternion  $q^{(0)} = 1 + 0i + 0j + 0k$ .
- 4) Convert three-axis gyro measurements to  $w_i = (w_{ix}, w_{iy}, w_{iz})$  instantaneous rotation quaternion as

$$q_{i\Delta} = q_i \left[ \Delta t \|\vec{w}_i\| t, \quad \frac{\vec{w}_i}{\|\vec{w}_i\|} t \Delta t \right] \quad (11)$$

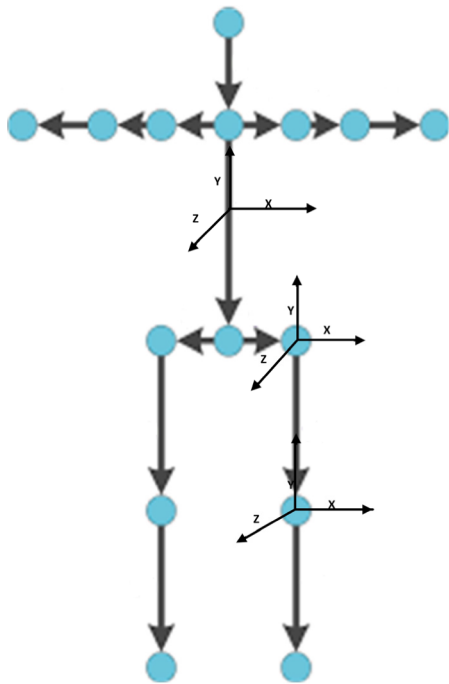


**Fig. 6.** Human coordinate system for three joints (thoracic, hip, and knee).

**TABLE I**  
NORMAL KNEE ROM (RANGE OF MOTION) REQUIRED FOR SOME ADL

Activity	ROM in Degree
Walking	0 – 65°
Climbing Up Stairs	0 – 85°
Descending Stairs	0 – 90°
Sitting Down	0 – 90°
Standing Up from Sitting	0 – 95°
Tying Your Shoelace	0 – 105°
Picking An Object Up from The Floor	0 – 75°
Riding A Bike	0 – 115°
Squatting	0 – 115° minimum
Sitting Cross Legged	0 – 115°

where

$\|\vec{w}_i\|$  is the angle;  
 $(\vec{w}_i / \|\vec{w}_i\|)$  Rotation axis.

We integrate as

$$q_w^{(t+\Delta t)} = q^{(t)} q_{\Delta t}. \quad (12)$$

Integrated gyro rotation quaternion  $q_w^{(t+\Delta t)}$  represents rotation from the body to the world frame, from (12) we have

$$q_u^{(\text{world})} = q_w^{(t+\Delta t)} q_u^{\text{body}} q_w^{(t+\Delta t)-1} \quad (13)$$

$q^{(t)}$  Last gyro measure.

We can write

$$q_{\text{new}} = R(q_{\text{gyro}}) q_{\text{old}} \quad (14)$$

where

- $R$  rotation matrix calculated as in (13);
- $\Delta$  instantaneous measured data from IMU;
- $i$  joint number; 1, 2, and 3.

To calculate rotation angle (pure quaternion) from (7)

$$w_i = \sqrt{w_{ix}^2 + w_{iy}^2 + w_{iz}^2}. \quad (15)$$

From (12), (13), (15), and (16), we can write

$$q_{\text{tha-new}} = R(q_{\text{gyro}}) q_{\text{tha-old}} \quad (16)$$

$$q_{\text{hip-new}} = R_{\text{hip}}(q_{\text{gyro}}) q_{\text{hip-old}} \quad (17)$$

$$q_{\text{knee-new}} = R_{\text{knee}}(q_{\text{gyro}}) q_{\text{knee-old}} \quad (18)$$

$$\beta = \sqrt{w_x^2 + w_y^2 + w_z^2} \quad (19)$$

$$\psi = \sqrt{w_x^2 + w_y^2 + w_z^2} \quad (20)$$

$$\gamma = \sqrt{w_x^2 + w_y^2 + w_z^2}. \quad (21)$$

**4) Phase Three (Prediction Algorithm):** In this phase, the prediction algorithm of fall occurrence is presented.

*a) Logistic Regression Model:* The mathematical prognostication scheme was formulated with the aid of logistic regression. Logistic regression entails projecting the existence or nonexistence of an outcome based on the values of forecast variables via statistical analysis. Logistic regression's flexibility in accommodating diverse predictor variable types, such as continuous, discrete, or a blend of both, obviates the need for adherence to normal data assumptions [24]. In this study, the dependent variable selected to represent an elderly fall event was binary, with occurrence or nonoccurrence signified by values of 0 and 1. For each independent variable, including joint angles such as the thoracic, hip, and knee joint angles, logistic regression generates coefficients. These calculated coefficients function as weights within a mathematical equation, used by a decision-making algorithm to calculate the probability of an elderly person experiencing a fall. Specifically, (22) depicts the logistic regression function, which determines the likelihood of a fall occurrence in the elderly population

$$p(x) = \frac{e^{(\beta_0 x + \beta_1 x_1 + \beta_2 x_2 + \dots + \beta_n x_n)}}{1 + e^{(\beta_0 x + \beta_1 x_1 + \beta_2 x_2 + \dots + \beta_n x_n)}}. \quad (22)$$

In the cited equation, the probability  $P(x)$  of an elderly person experiencing a fall event is calculated as a function of multiple independent variables, as represented by  $x_i$ , ( $i = 1, 2, 3, \dots, n$ ) here. The function includes a constant intercept term, marked by “beta zero”  $\beta_0$ , and coefficients, symbolized here as “betas”  $\beta_i$ , ( $i = 0, 1, 2, \dots, n$ ), representing the effect size of each independent variable, on the likelihood of a fall. Maximum likelihood estimation was utilized in computing the values of the model’s intercept and coefficients, marked as  $\beta_0$  and  $\beta_i$ , respectively, as described in [25]. The calculation was performed using the values of the independent variables, namely, the angles of the thoracic, hip, and knee joints, in combination with the state of the dependent variable. To calculate the body center using the probability function  $P(x)$  for fall events, where  $P(x)$  is a function of multiple

independent variables, including a constant intercept term (beta zero) and coefficients (betas), you would need to provide the specific formula or equation representing this probability function.

Given the varying structural compositions and joint types, different joint structures allow for different DOF and rotational ranges. Specifically, the hip joint functions as a universal joint and offers three rotational axes. The range of motion for different movements of the hip joint varies. Internal rotation has an approximate range of  $0^\circ$ – $50^\circ$ , while external rotation ranges from  $0^\circ$  to  $40^\circ$ . Forward flexion can typically range between  $0^\circ$  and  $140^\circ$ . In contrast, the extension allows for movements only up to  $10^\circ$  beyond the anatomical position. Adduction and abduction movements have a typical range of  $0^\circ$ – $30^\circ$  [8].

The thoracic flexion (forward) movement has a range of motion is about  $20^\circ$ – $45^\circ$ , the extension (backward) movement has a range of motion of about  $25^\circ$ – $45^\circ$ , and the lateral flexion movement has a range of motion of about  $20^\circ$ – $40^\circ$ .

A fully straight knee joint will measure  $0^\circ$ , and a fully bent knee will have at least degrees of flexion  $135^\circ$ , internal knee rotation  $10^\circ$ , and external knee rotation  $30^\circ$ – $40^\circ$ , depending on the size of the leg. In human joint kinematics, the point at which the calf pushes against the thigh is considered the limit beyond which hyperextension is deemed normal. Moreover, the model employed in this study leveraged the joint angles of the thoracic, hip, and knee joints to compute and determine the stature of elderly individuals, as stated previously [7] (Fig. 3).

To differentiate a change in walking motion from a fall based on several factors, including the severity of the alteration, the magnitude of the change, stability, and recovery. The people have a natural tilt in their regular walk, which may further alter after having a meal. We consider these variations in walk motion to differentiate them from a fall. In this article, we consider the magnitude of the changes in walk motion, we calculate the magnitude (15); the angles of tilt for the thoracic, the thigh, and the knee equations (19, 20, and 21). A natural tilt in the regular walk may be a gradual and subtle change that occurs consistently throughout the walking pattern. On the other hand, a fall involves a sudden and significant change in body position or orientation, usually resulting in uncontrolled descent or collapse. A slight tilt or alteration in gait after a meal is a normal physiological response and may not necessarily indicate a fall. However, if the change in motion is more pronounced or extreme, it could be an indication of a fall. Table I shows the knee ROM.

To calculation of the center of the body using IMU sensors can vary depending on the specific method used. However, one approach is to use a combination of accelerometer, gyroscope, and magnetometer data to estimate the orientation and then use this information to calculate the position of the center of mass (CoM). This can be done using machine learning techniques based on IMU data.

The assumption of defining the center of a person at the center of the body may vary from person to person. In certain applications and scenarios, we train a system using a logistic

regression model, and the actual data sensors were collected by using IMU9250 sensors by the authors in [26]. It is generally known that inertial sensors are small, lightweight, and portable, which makes them convenient for use in various settings. They can also provide real-time data on movement and orientation, which can be useful for monitoring and analyzing human motion. Additionally, inertial sensors can be less expensive than other motion capture systems, which can make them more accessible to researchers.

The method used in this study to estimate the CoM of the human body was based on the body-mounted IMU (BM-IMU) approach [27] based on logistic regression. This method involved attaching three IMUs to the thoracic, the thigh, and the knee of the elderly people, and using the acceleration and angular velocity data from the IMUs to compute the CoM position. By using logistic regression, we obtained function that can find the center of the body in term of some independent variables as (acceleration, the angular velocity, and orientation).

*b) Decision-Make Algorithm:* The decision-making algorithm was created to compute the likelihood of an elderly fall, classify activity, and generate a warning action. The steps below demonstrate how the presented algorithm determines the occurrence of elderly falls and makes the appropriate decision. An algorithm to compute elderly fall occurrence probability.

#### Classifying the ADL (fall, no-fall):

##### Step 1: Inputs.

Read (read the data sensor1thoracic).  
Read (read the data sensor 2 hip).  
Read (read the data sensor 3 knee).  
Read (data sensors every 1 s).

##### Step 2: Converting the sensors data to quaternions.

Update the data.

##### Step 3: Compute: Thoracic angle.

The angle between the thoracic and reference (center hip), [rotation angel  $\psi_i$  ( $i = 0, 1, 2, 3, \dots, n$ )].

##### Step 4: Compute: Hip angle.

The angle between hip and knee), [rotation angel  $\gamma_i$  ( $i = 0, 1, 2, 3, \dots, n$ )].

##### Step 5: Compute: Knee angel.

The angle between knee and foot (rotation angel  $\varphi_i$  ( $i = 0, 1, 2, 3, \dots, n$ )).

##### Step 6: Compute $p(x)$ according to (23).

##### Step 7: Classifying the output.

Classifying the output into 0, 1.

If  $p(x)$  1 no-fall end.

If  $p(x)$  0 fall.

Wait for 3 s send a message and go to step 2.

### III. MODEL EVALUATIONS AND PERFORMANCE ANALYSIS

#### A. Logistic Regression Model Development

To begin evaluating the issue of human falls by using the proposed mathematical model, we looked at existing datasets that contained falling, and ADL data. To evaluate the solution on same basis needs to be tested on same scenario, there is

a readymade dataset used called Inertial Measurement Unit Fall Detection Dataset (IMU) that was previously created [26]. The experimental results of the evaluation model utilizing the MATLAB 2022 a software are represented in this section. The system requirements for training are an Intel Core i5 processor, a 64-bit processor, a single CPU, and 32 GB of RAM, and SPSS V.23 software was used to calculate the parameters of the logistic regression model.

### B. Performance Evaluation

Several metrics that are used to analyze the performance of the proposed model for fall detection in the elderly are accuracy, precision, recall (Sensitivity), specificity, and the execution time latency ( $\varepsilon T$ ) on the IMU dataset. These metrics are defined with their mathematical expressions. The collected data comprises two distinctive class labels, namely, Fall and Non-Fall, each bearing a distinct sample size. Each of these class labels functions as a unique data instance and is employed to calculate the metrics, where classification efforts aim to accurately categorize them into true positive (TP), false positive (FP), true negative (TN), or false negative (FN) groups. Finally, a comparison with other techniques helps to determine how effective the logistic regression technique is resolved by comparison with existing methods

$$\text{Accuracy} = \frac{\text{TP} + \text{TN}}{\text{TP} + \text{TN} + \text{FP} + \text{FN}} \quad (23)$$

$$\text{Sensitivity} = \frac{\text{TP}}{\text{TP} + \text{FN}} \quad (24)$$

$$\text{Specificity} = \frac{\text{TN}}{\text{TN} + \text{FP}} \quad (25)$$

$$\varepsilon T = T_{\text{train}} + T_{\text{test}}. \quad (26)$$

### C. IMU Dataset

To validate the proposed method, we have used a standard IMU Data Set. The data used in the analysis were collected via MIU sensors implanted at various sites throughout participants' bodies [26]. The dataset was collected with the help of seven MPU wearable sensors from ten healthy young adults, aged between 22 and 32, with an average age of 26.6 years and a standard deviation of 2.8 years. All participants were Simon Fraser University students, and the university's Research Ethics Committee approved the research protocol. Prior to the experiment, each participant provided written consent. The experiment involved the observation of seven types of falls, five types of near-falls, and eight ADLs. Participants who experienced slipping, tripping, being struck or bumped, losing balance due to a misstep or cross-step, or losing balance while getting up from a chair all managed to successfully recover it during the near-fall trials. The ADLs comprised walking normally, standing quietly, rising from a chair, lowering oneself to a seat, lowering oneself to a lying position, picking something up off the ground, climbing stairs, and descending stairs. The study design ensured that each fall and non-fall scenario was given equal weight by having each participant simulate three repeated trials for each category. There were 210 falls, 150 near-falls, and 240 ADLs as a

**TABLE II**  
IMU DATASET (NUMBER OF PARTICIPANTS 10)

Falls	Non-falls		Number of trials
	Near-falls	ADLs	
Slips	Slips	Walking	3
Trips	Trips	Standing quietly	3
The incorrect shift of body-weight due to Misstep	Hit and bump by another person	Rising from sitting	3
Incorrect shift of bodyweight while rising from a chair	Incorrect shift of bodyweight while rising from a chair	Descending from standing to sitting	3
Incorrect shift of bodyweight while descending	Incorrect shift of bodyweight while descending	Descending from standing to lying	3
Collapse/ Loss of consciousness		Picking up an object from the ground	3
		Ascending stairs	3
		Descending stairs	3

**TABLE III**  
PARAMETER OF LOGISTIC REGRESSION MODEL

Independent variable	Logistic regression coefficient( $\beta$ )	Std. Error	Significant Probability
Thoracic angle	0.034	0.018	0.046
Thigh angle	0.153	0.012	0.028
Knee angle	0.193	0.027	0.030

consequence of this. The near-falls and ADLs were combined into a singular "non-falls" category for the purposes of fall classification. Trials that ended in successful balance recovery were labeled as "near-fall" events, while trials resulting in falls were labeled as "fall" events. For fall trials, participants were not given any instructions regarding the direction in which they should fall, except in cases where they lost consciousness or collapsed, in which case they were asked to fall straight down. During each trial, the researchers captured the body kinematics data using seven triaxial accelerometers (Opal model, APDM Inc., Portland, OR) positioned on both ankles and thighs, and at the waist, sternum, and head's anterior aspect. The data were collected at a rate of 128 Hz for 15 s per trial and transferred directly to a computer for storage and later analysis. The activities are used in this paper shown in Table II. Among the total ten people, we used four people's data for training and the remaining one for the test.

Based on the data presented in Table III, it becomes evident that the standard error (Std-Error) values were below 0.5, signifying their low magnitude. This indicates that the predictions are quite accurate and close to the eventual outcomes. Another parameter observed in Table III is the significance probability, which validates the influence of independent variables on elderly fall prediction. If the

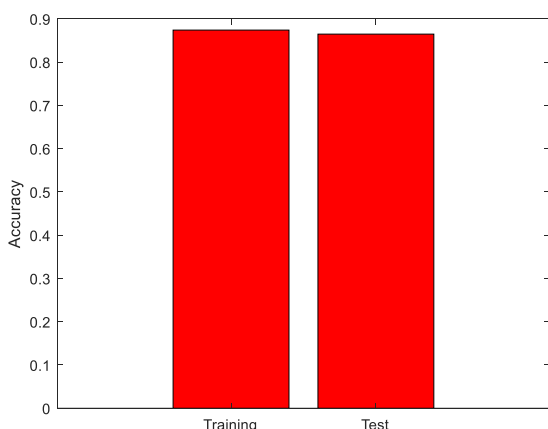


Fig. 7. Classification Accuracy Analysis.

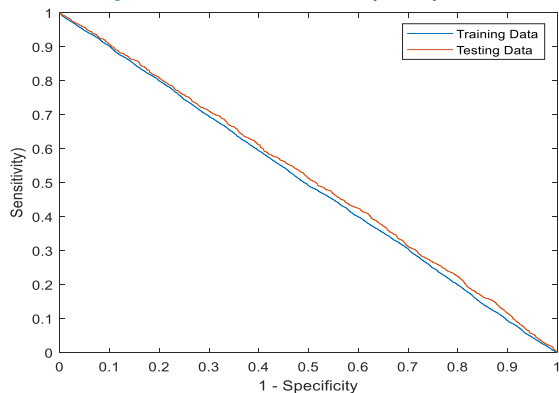


Fig. 8. ROC curve for training and testing IMU dataset.

significance probability is less than 0.05, it means that the independent variable has a statistically significant impact on elderly falls [28]. The results indicated that the thoracic angle, thigh angle, and knee angle possessed significant probability values in the range of (0.028–0.046), thereby statistically influencing the occurrence of elderly falls. As a result, these three independent variables (thoracic angle, thigh angle, and knee angle) were included in the model. Based on these useful independent variables and their parameters, the logistic regression model was constructed.

#### IV. PERFORMANCE ANALYSIS

This article proposes a sophisticated mathematical model for fall detection prediction in elderly individuals to reduce fall incidents. The model utilizes three IMU sensors and leverages logistic regression for accurate fall detection and prediction. Moreover, it incorporates a decision-making algorithm to classify elderly activities as fall or no-fall. The dataset used to evaluate the model is discussed in Section III-C. The logistic regression process yields model coefficients and additional statistical parameters, as depicted in Table III. The standard errors of the model coefficients range from 0.012 to 0.027, indicating high precision and close predictions to the actual outcomes. The Wald statistics parameter assesses the significance probability for all independent variable coefficients ( $\beta$ ). The significant probability values lie within the range of (0.028–0.046), indicating that all independent variables have statistically significant effects on elderly fall occurrence. These statistical results confirm the model's

robustness. Hence, three independent variables (slope angle, rainfall rate, and temperature variation) are included in the model.

The model's predictive abilities are evaluated using performance metrics like the area under the ROC curve (AUC), sensitivity, specificity, and accuracy. The overall prediction accuracy of the logistic regression model is 88% and 87.75%, respectively, during training and testing (Fig. 7), with an execution time latency of 0.0668 s. During model training and testing, the AUC values in the ROC curve (Fig. 8) are approximately 0.853 and 0.903, respectively. The average sensitivity during training and testing is 70.4% and 71.4%, respectively, demonstrating the model's favorable sensitivity in predicting elderly fall detection. The average specificity during training and testing is 75.3% and 75.5%, respectively.

#### V. CONCLUSION

This article presented a mathematical model to predict the occurrence of falls in elderly people or patients. The model developed was based on HBK and consists of two algorithms: a prediction probability of fall occurrence algorithm and a decision-making algorithm to decide the human status (ADL or fall); and evaluated using IMU dataset and show good outcomes in differentiate between elderly fall and non-fall. Quaternion was used to present the human body motion to the reference. Because of the simple calculations and limited memory space of using quaternions, the model can be implemented in real-time, both offline and online. Using the hip center joint as a reference, we calculated the joint angle for one reference and created separate coordinate systems for each joint in the T-pose skeleton. Due to the simple calculation and use of quaternions, which have advantages over Euler angles and the rotation matrix in less memory storage, we can implement the model in real life offline or online. The model can be used for a rigid body motion attitude because the quaternion does not have a singularity, it is capable of describing a full attitude, and the process of utilizing it does not involve a significant number of operations involving trigonometric functions.

#### REFERENCES

- [1] F. A. S. F. de Sousa, C. Escriba, E. G. A. Bravo, V. Brossa, J.-Y. Fourniols, and C. Rossi, "Wearable pre-impact fall detection system based on 3D accelerometer and subject's height," *IEEE Sensors J.*, vol. 22, no. 2, pp. 1738–1745, Jan. 2022, doi: [10.1109/JSEN.2021.3131037](https://doi.org/10.1109/JSEN.2021.3131037).
- [2] H. Adinanta, E. Kurniawan, and J. A. Prakosa, "Physical distancing monitoring with background subtraction methods," in *Proc. Int. Conf. Radar, Antenna, Microw., Electron. Telecommun.*, Nov. 2020, pp. 45–50, doi: [10.1109/ICRAMET51080.2020.9298687](https://doi.org/10.1109/ICRAMET51080.2020.9298687).
- [3] M. A. Naeem and S. F. Assal, "Development of a 4-DOF cane robot to enhance walking activity of elderly," *Proc. Inst. Mech. Eng., C, J. Mech. Eng. Sci.*, vol. 236, no. 2, pp. 1169–1187, Feb. 2019, doi: [10.1177/0954406219830440](https://doi.org/10.1177/0954406219830440).
- [4] C. W. Radcliffe, "Information useful in the design of damping mechanisms for artificial knee joints," *Prosthetic Devices Res. Project Inst. Eng. Res.*, Univ. California, Berkeley, CA, USA, Tech. Rep., Apr. 1950, no. 13.
- [5] J. V. Basmajian, "Muscles alive. Their functions revealed by electromyography," *Academic Med.*, vol. 37, no. 8, p. 802, 1962.
- [6] P. V. Karpovich and G. P. Karpovich, "Electrogoniometer: A new device for study of joints in action," *Fed. Proc.*, vol. 18, no. 79, p. 310, 1959.

- [7] S. C. Plagenhoef, "Methods for obtaining kinetic data to analyze human motions," *Res. Quarterly Amer. Assoc. Health, Phys. Educ. Recreation*, vol. 37, no. 1, pp. 103–112, Mar. 1966, doi: [10.1080/10671188.1966.10614742](https://doi.org/10.1080/10671188.1966.10614742).
- [8] H. Kang, Y. Li, D. Liu, and C. Yang, "Human kinematics modeling and simulation based on OpenSim," in *Proc. Int. Conf. Control, Autom. Inf. Sci. (ICCAIS)*, Oct. 2021, pp. 644–649, doi: [10.1109/ICCAIS52680.2021.9624647](https://doi.org/10.1109/ICCAIS52680.2021.9624647).
- [9] B. Açıs and S. Güney, "Classification of human movements by using Kinect sensor," *Biomed. Signal Process. Control*, vol. 81, Mar. 2023, Art. no. 104417, doi: [10.1016/J.BSPC.2022.104417](https://doi.org/10.1016/J.BSPC.2022.104417).
- [10] C. Dinh and M. Struck, "A new real-time fall detection approach using fuzzy logic and a neural network," in *Proc. 6th Int. Workshop Wearable, Micro, Nano Technol. Personalized Health*, Jun. 2009, pp. 57–60, doi: [10.1109/PHEALTH.2009.5754822](https://doi.org/10.1109/PHEALTH.2009.5754822).
- [11] S. Luo and Q. Hu, "A dynamic motion pattern analysis approach to fall detection," in *Proc. IEEE Int. Workshop Biomed. Circuits Syst.*, Dec. 2004, pp. 1–5.
- [12] J. Chen, K. Kwong, D. Chang, J. Luk, and R. Bajcsy, "Wearable sensors for reliable fall detection," in *Proc. IEEE Eng. Med. Biol. 27th Annu. Conf.*, Jan. 2006, pp. 3551–3554.
- [13] S. Badgjar and A. S. Pillai, "Fall detection for elderly people using machine learning," in *Proc. 11th Int. Conf. Comput., Commun. Netw. Technol. (ICCCNT)*, Jul. 2020, pp. 1–4, doi: [10.1109/ICCCNT49239.2020.9225494](https://doi.org/10.1109/ICCCNT49239.2020.9225494).
- [14] M. Aslan, A. Sengur, Y. Xiao, H. Wang, M. C. Ince, and X. Ma, "Shape feature encoding via Fisher vector for efficient fall detection in depth-videos," *Appl. Soft Comput.*, vol. 37, pp. 1023–1028, Dec. 2015, doi: [10.1016/J.ASOC.2014.12.035](https://doi.org/10.1016/J.ASOC.2014.12.035).
- [15] B. Galna, G. Barry, D. Jackson, D. Mhiripiri, P. Olivier, and L. Rochester, "Accuracy of the Microsoft Kinect sensor for measuring movement in people with Parkinson's disease," *Gait Posture*, vol. 39, no. 4, pp. 1062–1068, Apr. 2014.
- [16] J. Wadmare, D. Shah, C. Diwakar, and V. Bhanushali, "A vision based approach for fall detection system for elderly people," *SSRN Electron. J.*, May 2021, doi: [10.2139/SSRN.3867407](https://doi.org/10.2139/SSRN.3867407). [Online]. Available: <https://ssrn.com/abstract=3867407>
- [17] M. Kangas, I. Vikman, J. Wiklander, P. Lindgren, L. Nyberg, and T. Jämsä, "Sensitivity and specificity of fall detection in people aged 40 years and over," *Gait Posture*, vol. 29, no. 4, pp. 571–574, Jun. 2009.
- [18] S. O. H. Madgwick, A. J. L. Harrison, and R. Vaidyanathan, "Estimation of IMU and MARG orientation using a gradient descent algorithm," in *Proc. IEEE Int. Conf. Rehabil. Robot.*, Jun. 2011, pp. 1–7, doi: [10.1109/ICORR.2011.5975346](https://doi.org/10.1109/ICORR.2011.5975346).
- [19] M. A. Paparisabet, R. Dehghani, and A. R. Ahmadi, "Knee and torso kinematics in generation of optimum gait pattern based on human-like motion for a seven-link biped robot," *Multibody Syst. Dyn.*, vol. 47, no. 2, pp. 117–136, Oct. 2019, doi: [10.1007/s11044-019-09679-z](https://doi.org/10.1007/s11044-019-09679-z).
- [20] T. Teramae, T. Matsubara, T. Noda, and J. Morimoto, "Quaternion-based trajectory optimization of human postures for inducing target muscle activation patterns," *IEEE Robot. Autom. Lett.*, vol. 5, no. 4, pp. 6607–6614, Oct. 2020.
- [21] E. Demircan, "A pilot study on locomotion training via biomechanical models and a wearable haptic feedback system," *ROBOMECH J.*, vol. 7, no. 1, p. 19, Dec. 2020, doi: [10.1186/s40648-020-00167-0](https://doi.org/10.1186/s40648-020-00167-0).
- [22] K. R. Embry, D. J. Villarreal, R. L. Macaluso, and R. D. Gregg, "Modeling the kinematics of human locomotion over continuously varying speeds and inclines," *IEEE Trans. Neural Syst. Rehabil. Eng.*, vol. 26, no. 12, pp. 2342–2350, Dec. 2018, doi: [10.1109/TNSRE.2018.2879570](https://doi.org/10.1109/TNSRE.2018.2879570).
- [23] E. Palermo, S. Rossi, F. Marini, F. Patanè, and P. Cappa, "Experimental evaluation of accuracy and repeatability of a novel body-to-sensor calibration procedure for inertial sensor-based gait analysis," *Measurement*, vol. 52, pp. 145–155, Jun. 2014, doi: [10.1016/j.measurement.2014.03.004](https://doi.org/10.1016/j.measurement.2014.03.004).
- [24] S. Lee, "Application of logistic regression model and its validation for landslide susceptibility mapping using GIS and remote sensing data," *Int. J. Remote Sens.*, vol. 26, no. 7, pp. 1477–1491, Apr. 2005.
- [25] G. Tian, Y. Liu, and M. Tang, "Logistic regression analysis of non-randomized response data collected by the parallel model in sensitive surveys," *Austral. New Zealand J. Statist.*, vol. 61, no. 2, pp. 134–151, Jun. 2019.
- [26] O. Aziz, M. Musngi, E. J. Park, G. Mori, and S. N. Robinovitch, "A comparison of accuracy of fall detection algorithms (threshold-based vs. machine learning) using waist-mounted tri-axial accelerometer signals from a comprehensive set of falls and non-fall trials," *Med. Biol. Eng. Comput.*, vol. 55, no. 1, pp. 45–55, Jan. 2017, doi: [10.1007/s11517-016-1504-y](https://doi.org/10.1007/s11517-016-1504-y).
- [27] G. Pavei, F. Salis, A. Cereatti, and E. Bergamini, "Body center of mass trajectory and mechanical energy using inertial sensors: A feasible stride?" *Gait Posture*, vol. 80, pp. 199–205, Jul. 2020, doi: [10.1016/j.gaitpost.2020.04.012](https://doi.org/10.1016/j.gaitpost.2020.04.012).
- [28] N. B. Raja, I. Çiçek, N. Türkoğlu, O. Aydin, and A. Kawasaki, "Landslide susceptibility mapping of the sera river basin using logistic regression model," *Natural Hazards*, vol. 85, no. 3, pp. 1323–1346, Feb. 2017, doi: [10.1007/s11069-016-2591-7](https://doi.org/10.1007/s11069-016-2591-7).



**Safa Hussein Mohammed** received the B.Sc. degree in electronics engineering (communication) from Al-Neelan University, Khartoum, Sudan, in 2008, and the M.Sc. degree in electronics engineering (communication) from the Sudan University of Science and Technology (SUST), Khartoum, in 2015. She is pursuing the Ph.D. degree with the School of Electronics and Information, Northwestern Polytechnical University, Xi'an, China.

She is a Lecturer with the Electrical Technological Department, Kosti Technological College, Sudan Technological University, Khartoum. Her research interests are in the IoT, electronics embedded systems, and AI.



**Yangyu Fan** received the M.S. degree in electromechanical engineering from the Shaanxi University of Science and Technology, Xi'an, China, in 1992, and the Ph.D. degree in acoustics signal processing from Northwestern Polytechnical University, Xi'an, in 1999.

He is a Professor with the School of Electronics and Information, Northwestern Polytechnical University. His research interests include image processing, pattern recognition, and virtual reality.



**Guoyun Lv** is an Associate Professor with the School of Electronics and Information, Northwestern Polytechnical University, Xi'an, China. His theoretical research direction entails voice and video image processing, and virtual reality. His engineering research direction entails embedded operating systems, embedded systems, the Internet of Things, and airborne and missile-borne test technology. From 2008 to 2010, he was engaged in postdoctoral research in the postdoctoral mobile station

at the School of Electronics and Information, Northwest University of Technology, Xi'an. His postdoctoral research direction entails signal and information processing, speech and image processing, virtual reality, embedded systems and high-speed signal processing, pattern recognition, and measurement and control technology.



**Shiya Liu** is the Director of the Content Production Center of Virtual Reality, Beijing, China, and the Qingdao Star Shark Virtual Reality Technology Research Institute, a Researcher of the United Nations Institute of Digital Economy, a member of the Information and Communication Economy, and an Expert Committee of the Ministry of Industry and Information Technology. Her research interests include the integration, innovation, and application of high and new technologies in the field of electronic information and communication, such as VR/AR, 4K/8K, AI, 5G, and microelectronics.

Authorized licensed use limited to: Ariel University. Downloaded on December 08, 2024 at 20:37:11 UTC from IEEE Xplore. Restrictions apply.